Dynamic Maximum Power Point Tracker for Photovoltaic Applications

Pallab Midya
Motorola, Inc., Corporate Development Labs
Schaumburg, Illinois

Philip T. Krein Robert J. Turnbull Robert Reppa Jonathan Kimball
University of Illinois
Department of Electrical and Computer Engineering
Urbana, Illinois 61801

Abstract — A dynamic process for reaching the maximum power point of a variable source such as a solar cell is introduced. The process tracks maximum power nearly cycle-by-cycle during transients. Information from the natural switching ripple instead of external perturbation is used to support the maximizing process. The method is globally stable for dc-dc converters, provided that switch action is present. A prototype boost converter that uses this method for control can follow power transients on time scales of a few milliseconds. This performance can be achieved with a simple analog control structure, which supports power processing with minimum loss.

I. Introduction

Background

Power from many alternative energy sources is highly variable — sensitive to temperature, time drift, component variation, and environmental conditions. Solar cell output, for example, is a strong function of illumination and temperature. In most such sources, it is desirable to extract the highest possible power at any moment. Power output is not usually a monotonic function of control variables, however, so controls derived from linear system methods cannot track the peak power level.

The issue of power tracking has been addressed previously with perturbation techniques [1]: an interface converter adjusts the source voltage V_s or current I_s and monitors the power P_s. A microprocessor or similar hardware compares various operating points and selects for maximum power. The perturbation process operates continuously to keep the power near its maximum. The process in effect serves as a way to measure a derivative such as $\partial P_s/\partial V_s$, then operate the interface converter such that $\partial P_s/\partial V_s \approx 0$. It is hard to implement the process without an active control and memory because of the sign of $\partial P_s/\partial V_s$: above the optimum voltage, $\partial P_s/\partial V_s < 0$, while below the optimum $\partial P_s/\partial V_s > 0$. Information from off-optimum operating points is necessary to determine the derivative sign.

In most implementations, the perturbation method uses average voltage, power, or current, and perturbs the converter duty ratio to provide information about the derivatives. The process is relatively slow, since good signal to noise ratio requires averages over many cycles. Systems reported in the literature [2-4] follow the maximum power point at time scales of seconds or longer.

Often, an approximation is used for the solar cell power P_s required in the perturbation approach. In [4], for example, a maximum power-point tracker (MPPT) charges a battery pack from a solar panel. The battery voltage is relatively stiff, so battery charging current serves as a useful measure of P_s.

In this paper, upper-case quantities such as P_s refer to average values in a converter, while lower-case values such as v_s refer to the instantaneous time-varying signals. Ripple signals are important, and are indicated with a tilde. The optimum points are denoted v_{opt}, etc.

Switching Ripple as an Alternative Perturbation

The perturbation process is inconvenient, slow, and fundamentally sub-optimal in the sense that the converter must be perturbed from the desired point for control purposes. However, consider that an MPPT is normally a switching power converter that exposes the source to low-level ripple. *The ripple can be considered a dynamic perturbation.* In this paper, it is shown how to make use of ripple itself to obtain maximum power tracking in a photovoltaic application. No extra perturbation is needed, so the technique keeps converter operation at the optimum point. Ripple measurement allows tracking on a time scale of only a few switching periods. The approach computes a dynamic measure of $\partial p_s/\partial i_s$ or $\partial p_s/\partial v_s$ from voltage and current. The information is used in a PWM feedback loop in a conventional dc-dc converter. An experimental implementation uses a simple analog control circuit, and tracks the maximum power of a solar panel over a bandwidth approaching 1 kHz.

II. Objectives and Characteristics

In a photovoltaic application, the following objectives can be identified:

0-7803-3500-7/96/$ 5.00 © 1996 IEEE

- Maintain the source power as close as possible to its (optimum) maximum point, i.e. $P_s = P_{opt}$. A *tracking effectiveness* can be defined as the ratio P_s/P_{opt}
- Provide very high conversion efficiency for the converter, so that the ratio $P_{out}/P_s \approx 1$.
- Maintain tracking over wide variations, such as illumination levels with 20 dB or more of dynamic range and wide temperature swings.
- Provide an output interface compatible with battery charging requirements.

The application motivating the work presented here is a solar-powered vehicle. In this mobile system, fast dynamic response takes full advantage of rapidly changing conditions. It is critical not to sacrifice one objective in favor of another. The approach described in this paper improves tracking effectiveness compared to previous methods, supports high efficiency because of the simple control structure, and follows rapid changes in conditions over a wide dynamic range.

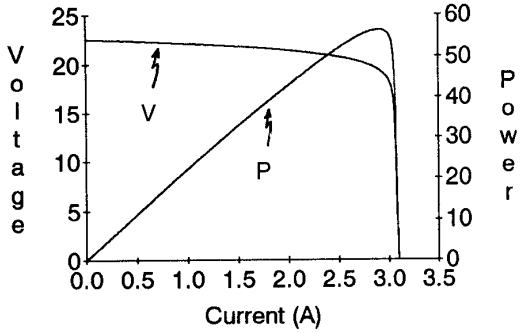

Fig. 1. Characteristics of a silicon solar panel.

The action of a typical single-crystal silicon solar panel is illustrated in Fig. 1. The figure shows P_s vs. I_s and V_s vs. I_s for nominal conditions given a series string of 40 cells, each formed as a four inch full wafer. The maximum power occurs at the point $\partial P_s/\partial I_s = 0$. Solar cells show a unique global maximum point; there are no suboptimal local maxima along the smooth curve in Fig. 1. In Fig. 2, the effects of external variation on the characteristic curve are shown. Fig. 2a shows voltage-current behavior parametrized by illumination level. The short-circuit current is approximately a linear function of illumination intensity. The 100% level represents a standard intensity of 1 kW/m². Fig. 2b shows voltage-current behavior parametrized by temperature. Temperature alters the cell voltage at about -0.4%/°C [5]. This reduces V_s very significantly in operation: a good quality cell is about 15% efficient at converting light to electricity, so 85% of incident light heats the solar cell rather than contributing to electrical output. An effective MPPT needs closed-loop control to correct for changes in both illumination and temperature. Static settings such as constant voltage, constant current, or even constant impedance will not be effective under both types of variation.

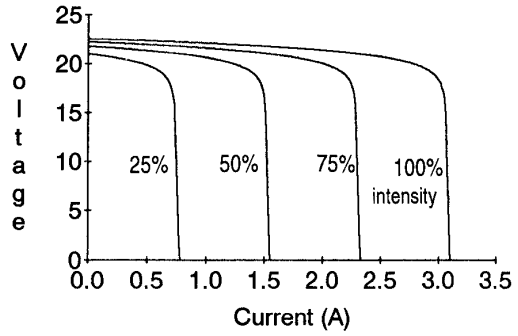

a) Illumination effect

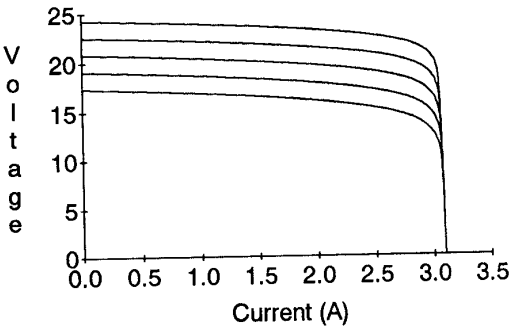

b) Temperature effect

Fig. 2. Cell behavior as a function of illumination and temperature.

III. The Dynamic Approach

Ripple correlation

Consider a solar panel connected to a dc-dc converter. As the switches operate, the panel is exposed to current and voltage ripple. If the characteristic curve in Fig. 1 is taken as a dynamic V-I model, the ripple will cause the input to move back and forth along the characteristic. In Fig. 3, the instantaneous behavior of v_s, i_s, and p_s is illustrated for three cases: current below that for the optimum power, $i_s < i_{opt}$, current near the optimum, and current above the optimum. This behavior would be similar for any dc-dc converter topology.

The cell behavior is reflected in both the shapes and phase relationships. In particular, notice that the phase relationships between p_s and either v_s or i_s change through the optimum point. Correlation is one convenient way to obtain relative phase information. The maximum power point can be tracked

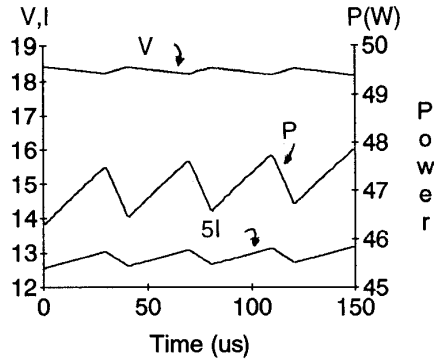

a) Operation at $i_s < i_{opt}$

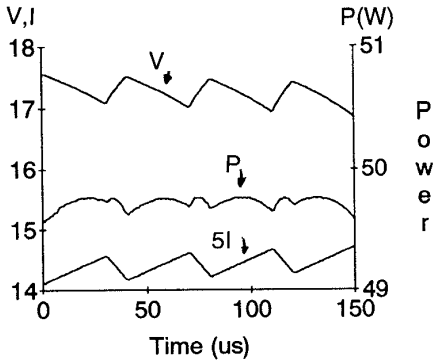

b) Operation at $i_s \approx i_{opt}$

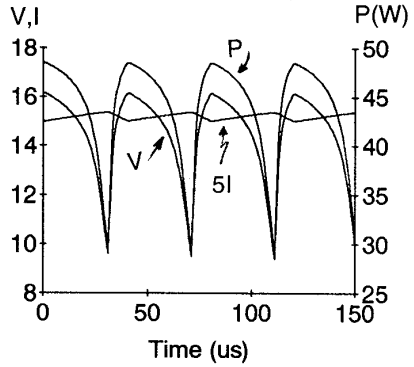

c) Operation at $i_s > i_{opt}$

Fig. 3. Ripple voltage, current, and power for various operating points.

by following the correlation between p_s and either the voltage or current ripple waveform [6]. A heterodyne process can be used or a more formal correlation can be computed. Let us denote the time derivative with a prime symbol ('). The products $p_s'v_s'$ or $-p_s'i_s'$ give the necessary phase information: on the average, $p_s'v_s'$ or $-p_s'i_s'$ will be negative if $i_s < i_{opt}$, positive if $i_s > i_{opt}$, and zero when the maximum power point is being tracked. We use the product $p_s'v_s'$ as the basis for control, because the current is so close to constant above the optimum value that the current ripple becomes very small just beyond the desired operating point. It is important to observe that the product $p_s'v_s'$ is a chain rule derivative, equal to dp_s/dv_s. Thus the ripple product is a measure of $\partial P_s/\partial V_s$. If the product is driven to zero, power will be maximized.

An actual implementation does not require measurement of power. By the chain rule,

$$p_s'v_s' = \left(i_s v_s' + v_s i_s'\right) v_s' \tag{1}$$

For control flexibility, a gain parameter α is added, to give

$$p_s'v_s' = \left(\alpha i_s v_s' + v_s i_s'\right) v_s' \tag{2}$$

The time integral of (2) represents a correlation function $c_P(t)$. This function can be used directly as a duty ratio control input for the converter. The integral control approach will drive (2) to zero, and therefore tracks p_{opt} continuously and quickly.

The waveforms in Fig. 3 suggest an alternative control formulation. If ac-coupled measurements of i_s and v_s are made, written as $\tilde{i}_s$ and $\tilde{v}_s$, then the phase information is contained in $\tilde{p}_s\tilde{v}_s$. The ac portion of the power is the product $(V_s + \tilde{v}_s)(I_s + \tilde{i}_s)$ less the dc portion V_sI_s. This product can be written as

$$\tilde{p}_s\tilde{v}_s = (V_s\tilde{i}_s + I_s\tilde{v}_s)\,\tilde{v}_s \tag{3}$$

This is just like (1), except that ac coupled signals have been substituted for time derivatives. The time integral of (3) can serve as a control signal. This simple method tracks the maximum power point continuously, just as c_P does.

Stability analysis

The correlation control c_P provides a monotonic function that has a constant value if the converter operates at the maximum power point. The duty ratio control input $d(t)$ is given by $d(t) = -kc_p(t)$. In this section, we consider the conditions required to ensure successful operation. Global stability can be proved with few restrictions.

The control law (with $\alpha = 1$) can be written as

$$d(t) = -k\int\frac{dp_s}{dt}\frac{dv_s}{dt}dt \tag{4}$$

The time derivative of power based on the chain rule can be written

$$\frac{dp_s}{dt} = \frac{\partial p_s}{\partial v_s}\frac{dv_s}{dt} \tag{5}$$

Substitution into (4) yields

$$d(t) = -k\int (v_s')^2 \frac{\partial p_s}{\partial v_s} dt, \quad \text{or} \quad d' = -k(v_s')^2 \frac{\partial p_s}{\partial v_s} \tag{6}$$

Stability relies on two basic assumptions: first, that there are no local maxima in P_s (or p_s) with respect to v_s; second, that there is always nonzero ripple in input voltage. The first assumption means that anywhere away from the absolute maximum power, $\partial p_s/\partial v_s$ is strictly nonzero. If this condition fails, then the duty ratio stops changing, latching on to a local maximum. In the solar cell system, experimental data shows no evidence of local maxima; if any were present in known locations, some method of restriction would be necessary to exclude these maxima from the operating region. The second assumption is, in general, true whenever the converter is switching. Since the voltage is always changing when the switches are active, $(v_s')^2$ is always strictly positive. The system will always be perturbed. In the implementation here, this second assumption is enforced by limiting the duty ratio, so that it can never be 0 or 100%.

Under these two assumptions, (6) has a unique equilibrium point: $d' = 0$ if and only if $\partial p_s/\partial v_s = 0$. It remains to show that this equilibrium point is stable. Disturbances to the system can be analyzed as if starting from some duty ratio d_{opt} corresponding to the optimum point v_{opt}, i_{opt}, and p_{opt}. The question of stability reduces to whether or not $p_s(t)$ approaches p_{opt} over time. As an example converter with nonlinear behavior, consider a boost converter. This circuit is shown with the power tracking control in Fig. 4. Ideally, the input and output voltage are related by the transistor duty ratio, such that $V_s = V_{out}(1 - d)$. Let the MOSFET have some on-resistance $R_{ds(on)}$. The diode exhibits a forward drop V_d, and resistance. For simplicity, let the diode resistance be $R_{ds(on)}$ as well. The input-output relationship becomes

$$V_s = R_{ds(on)} I_s + (1-D)(V_{out}+V_d) \tag{7}$$

The time derivative of (7) can be simplified to

$$V_s' = -\frac{d'(V_{out}+V_d)}{1 - R_{ds(on)}\dfrac{\partial i_s}{\partial v_s}} \tag{8}$$

As long as $\partial i_s/\partial v_s$ is always negative, as in solar cells, the derivative V_s' is negative with respect to d'. This fact is used to advantage in the Lyapunov stability analysis that follows.

Consider a cost function $J = P_{opt} - P_s$. Since P_{opt} is the maximum power, the function $J(t) \geq 0$. By the direct method of Lyapunov, if the time derivative $dJ/dt = -dP_s/dt$ is negative, the equilibrium point is stable. Disturbances to the system can be separated into two classes: changes to the load voltage and changes to the operating point P^{opt}. Starting from equilibrium, a step change in V_{out} will not change d initially. However, from (7) the value of V_s will make a step change owing to the change in V_{out}. Since a step change in V_s moves operation off the equilibrium point, at some time δt after a step change $\partial P_s/\partial V_s$ and d' are no longer zero. For a step increase in V_{out}, such as a power-on transient, there is a step increase in V_s. For $v_s > v_{opt}$, the derivative signs become

$$\frac{\partial P_s}{\partial V_s} < 0, \quad d' > 0 \tag{9}$$

From (8), this causes V_s to fall. The power therefore rises, and $dJ/dt < 0$. For a step decrease in V_{out}, there is an initial decrease in V_s. The solar cells exhibit a positive value of $\partial P_s/\partial V_s$ and the control creates a negative value for d'. From (8), the voltage V_s rises. The power therefore rises, and $dJ/dt < 0$. Any step change in V_{out} is followed by some transient in which J is caused to decrease, guaranteeing large-signal stability for this type of disturbance.

In some sense, a step change to the source is equivalent to a step change in the load. Change in illumination, for example moves the maximum power point from V_{opt} and P_{opt} to new values $V_{opt(2)}$, $P_{opt(2)}$. If the change in the source is fast relative to the time constant of the integrator for c_p, then V_s does not change instantaneously. At this point, either $V_s > V_{opt(2)}$ (equivalent to a step increase in V_{out}), or $V_s < V_{opt}$, and the situation is equivalent to a step decrease in V_{out}. In either case, the algorithm forces J to decrease with time, and large-signal stability is guaranteed.

IV. Implementation

Circuit and steady-state performance

The correlation control technique has little dependence on the form of the power converter. It can be used with any duty-ratio controlled dc-dc converter, or adapted for frequency adjustment in resonant converters. The boost converter and controller shown in Fig. 4 has been used in the solar vehicle application with excellent results. The circuit includes an overvoltage shutdown set to provide a battery charging limit. A duty ratio limit is set with a bias potential at the SG3526 input to ensure that switching always takes place to meet stability conditions. The circuit is hot-pluggable, and is suitable for use in a distributed system. In the solar vehicle application, 22 such units were used together for power tracking of multiple panels. This boost design uses nominal 20 V input and 72 V output, although the circuit has no special limitations on these operating parameters.

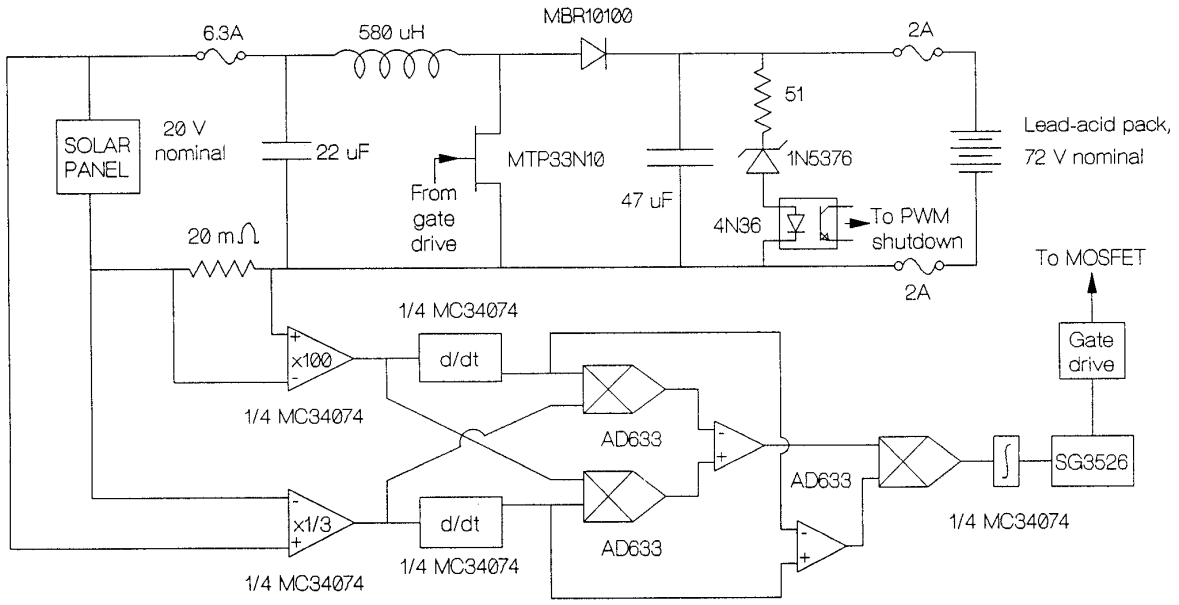

Fig. 4. Boost converter and analog controller for dynamic MPPT.

Table I lists tracking effectiveness results given a fixed output voltage and varying levels of illumination. The value of P_{opt} is determined by manual adjustment. Tracking effectiveness is limited only by controller precision, and

TABLE I. TRACKING EFFECTIVENESS AT VARIOUS ILLUMINATION LEVELS FOR BOOST MPPT.

V_{out}	I_{out}	P_{out}	$I_{out(opt)}$	$P_{out(opt)}$	Tracking effectiveness, $P_{out}/P_{out(opt)}$
64.86	0.094	6.10	0.096	6.23	0.979
64.86	0.141	9.15	0.142	9.21	0.993
64.86	0.192	12.45	0.193	12.52	0.995
64.86	0.259	16.80	0.259	16.80	1.00
64.86	0.316	20.50	0.316	20.50	1.00
64.86	0.385	24.97	0.385	24.97	1.00
64.86	0.454	29.45	0.456	29.58	0.996
64.86	0.506	32.82	0.513	33.27	0.986

Table I suggests that the method does indeed drive the converter to the maximum power point. Additional experiments on tracking effectiveness gave values of 98% or better for illumination levels between 10% and 100% and over cell temperatures ranging from 10°C to more than 70°C.

Power efficiency is a function of the converter design rather than the algorithm, since only a few low-power analog ICs are needed in the implementation. Typical conversion efficiency was about 96% for this circuit, including all control power.

Dynamic performance

The large-signal stability properties of the algorithm are very beneficial in practice. The converter can be connected to the cells or batteries without causing operating problems. The PWM IC in the converter provides the clock signal, so it is easy to guarantee continuous switch action. In this battery-based system, one issue is loss of the battery connection or the effect of fully charged batteries. In either case, the converter should shut off rather than continue to deliver maximum power to the output. This shutoff action is achieved with a zener diode and an optocoupler: if the output voltage exceeds the zener threshold, current will flow in the optocoupler diode, and the SG3526 chip is shut down. With the shutdown circuit in place, the converter cannot overcharge the batteries or overdrive the filter capacitors. The action has proved to be robust in long-distance drive tests.

Figs. 5 and 6 show dynamic performance of the boost circuit. In Fig. 5, the response to an input step is recorded. In Fig. 5a, an additional solar panel is switched in to step the maximum power point by 33%. The converter recovers to the optimum level in about 2 ms. Fig. 5b shows the response to an input power decrease. Again, the converter returns to the optimum point within about 2 ms. Fig. 6 shows the response to output voltage changes. Fig. 6a shows a 15% decrease in V_{out}. The response is a bit oscillatory, but the operating point recovers within 2 to 3 ms. Recovery is slower for the output voltage increase shown in Fig. 6b, most likely because of integrator tuning. In the figure, a 25% output voltage increase is tracked after 4-5 ms.

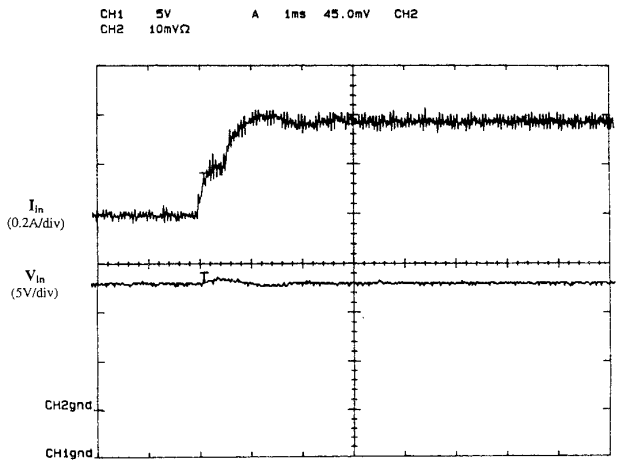

a) Step increase in input power.

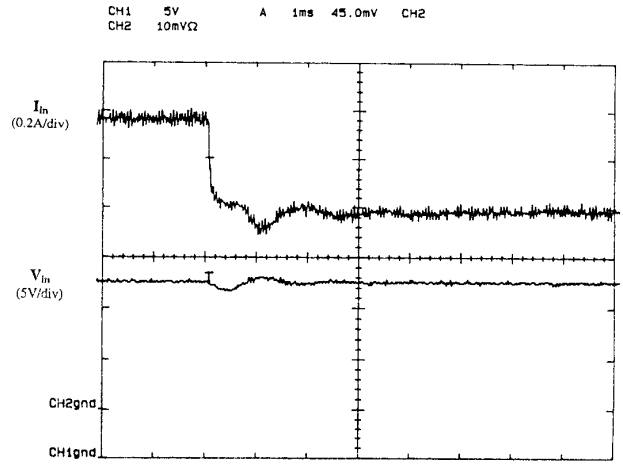

b) Step decrease in input power.

Fig. 5 Dynamic response to input power step.

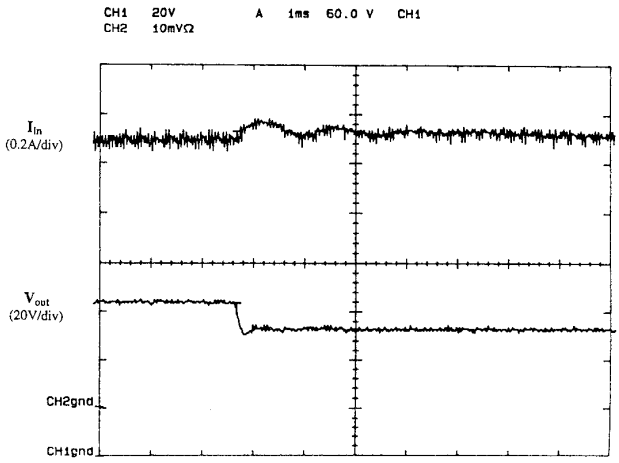

a) Step decrease in output voltage.

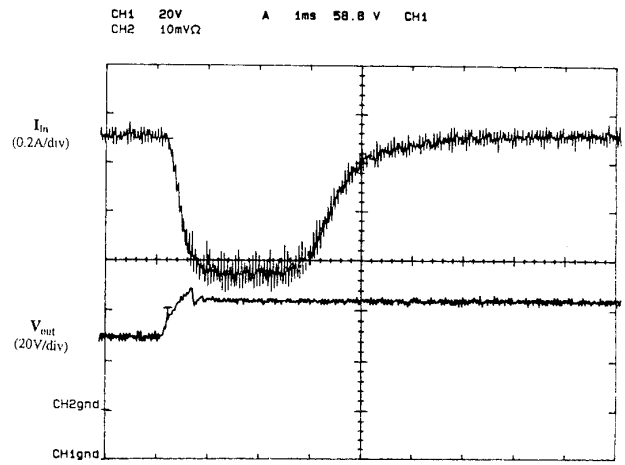

b) Step increase in output voltage.

Fig. 6 Response to output voltage transients.

Operating limitations

The correlation control method uses ripple to perturb solar cell operation. This technique has two fundamental limitations. First, the algorithm performance depends on signal-to-noise ratio. Ripple is easy to measure and process, but the method will not work well if very aggressive filtering is used to eliminate ripple. As a consequence, performance depends on switching frequency: high switching means low ripple, and possible trouble with the algorithm. In the circuit of Fig. 4, the switching frequency is about 15 kHz. The input filter of the boost converter imposes voltage ripple of about 0.1 $V_{peak\text{-}to\text{-}peak}$ on the solar cells, or about 0.6% of the nominal level of 20 V. This translates into a few tenths of 1% of power that is not used to advantage because of the ripple.

A second issue is the dynamic behavior of the solar cells. Like any P-N junction structure, cells exhibit a voltage-dependent capacitance. At high speeds, a dynamic V-I characteristic is observed. The waveforms of Fig. 3 are not

accurate when this happens because of phase shifts. The correlation control process is relatively robust to the capacitive cell current, because the current is in quadrature to the main terms in (2). In the correlation integral, the capacitive effect tends to average out.

V. Conclusion

A dynamic approach to power-point tracking has been described. The approach makes use of converter ripple as an alternative to external operating point perturbation. An implementation shows dramatic improvements in tracking effectiveness, transient performance, and dynamic range over previous MPPT methods. The improvements are made with a simple analog control loop added to a conventional dc-dc converter, and can be implemented at low cost.

References

[1] V. Vittorio, S. Corsi, L. Lambri, "Maximum power point tracker for photovoltaic plants," in *Proc. IEEE Photovoltaic Specialists Conf.*, 1982, pp. 507-512.

[2] F. Umeda, M. H. Ohsato, G. Kimura, M. Shioya, "New control method of resonant dc-dc converter in small scale photovoltaic system," in *Rec., IEEE Power Electronics Specialists Conf.*, 1992, pp. 714-718.

[3] J. H. R. Enslin, D. B. Snyman, "Combined low-cost high-efficient inverter, peak power tracker and regulator for PV applications," *IEEE Trans. Power Electronics*, vol. 6, no. 1, pp. 73-82, 1991.

[4] C. R. Sullivan, M. J. Powers, "A high-efficiency maximum power point tracker for photovoltaic arrays in a solar-powered race vehicle," in *Rec., IEEE Power Electronics Specialists Conf.*, 1993, pp. 574-580.

[5] M. Buresch, *Photovoltaic Energy Systems*. New York: McGraw-Hill, 1983.

[6] C. C. Hang, K. K. Sin, "On-line auto tuning of PID controllers based on the cross-correlations technique," *IEEE Trans. Industrial Electronics*, vol. 38, no. 6, pp. 428-437, 1991.